Chapter 1
Cardiac Physiology

Brian Feingold, Ricardo Munoz, and Ryan Flanagan

Abstract A basic understanding of cardiovascular physiology is fundamental to the comprehension of the conditions and pharmacologic mechanisms described throughout this Handbook. This chapter will provide an overview of cardiovascular physiology while highlighting the unique aspects of the neonatal and pediatric heart. While not intended to be an exhaustive review, the chapter should serve to familiarize the reader with concepts, such as cardiac structure and function, electrophysiology, shunt lesions, contractility, preload and afterload, and clinical measures of cardiac function, to be discussed in greater detail in other chapters.

B. Feingold, MD, MS
Department of Pediatric Cardiology,
Children's Hospital of Pittsburgh of UPMC, Pittsburgh, PA, USA

R. Munoz, MD, FAAP, FCCM, FACC
Cardiac Intensive Care Division, The Heart Institute,
Children's Hospital of Pittsburgh of UPMC,
University of Pittsburgh, Pittsburgh, PA, USA

R. Flanagan, MD (✉)
Division of Pediatric Cardiology, Department of Pediatrics,
Children's Hospital of Pittsburgh of UPMC, Pittsburgh, PA, USA

Department of Pediatrics, Womack Army Medical Center,
2817 Reilly Road, Fort Bragg, NC, USA
e-mail: ryanflanagan1@yahoo.com

R. Munoz et al. (eds.), *Handbook of Pediatric Cardiovascular Drugs*, DOI 10.1007/978-1-4471-2464-1_1,

Keywords Cardiac physiology • Dysrhythmias • Shunt lesions • Preload • Afterload • Contractility

A basic understanding of cardiovascular physiology is fundamental to the comprehension of the conditions and pharmacologic mechanisms described throughout this Handbook. With that goal in mind, this chapter will provide an overview of cardiovascular physiology while highlighting the unique aspects of the neonatal and pediatric heart. While not intended to be an exhaustive review, the chapter should serve to familiarize the reader with concepts to be discussed in greater detail in other chapters. For those seeking further knowledge, a list of more comprehensive sources is provided at the conclusion of this chapter.

1.1 Basic Cardiac Structure and Function

The human heart is in essence two pumps connected in series, delivering blood to the pulmonary and systemic circulations. It is comprised of two atria which receive venous blood, two ventricles which pump blood, valves which prevent the backflow of blood, and a conduction system which transmits the electrical impulses that drive cardiac activity. The electrical signal is propagated and converted to mechanical activity through a series of biochemical interactions which involve stereotyped ion fluxes (mainly Na^+, Ca^{++}, K^+) through voltage-gated ion 'pores' and downstream protein interactions. While inherited or acquired defects in these components may result in cardiac disease, these same mechanisms form the basis of pharmacologic therapies.

1.2 Electrophysiology

Rhythmic and coordinated contraction of the heart is accomplished by the propagation of an electrical impulse (action potential) in a precise manner (Fig. 1.1). Each action potential

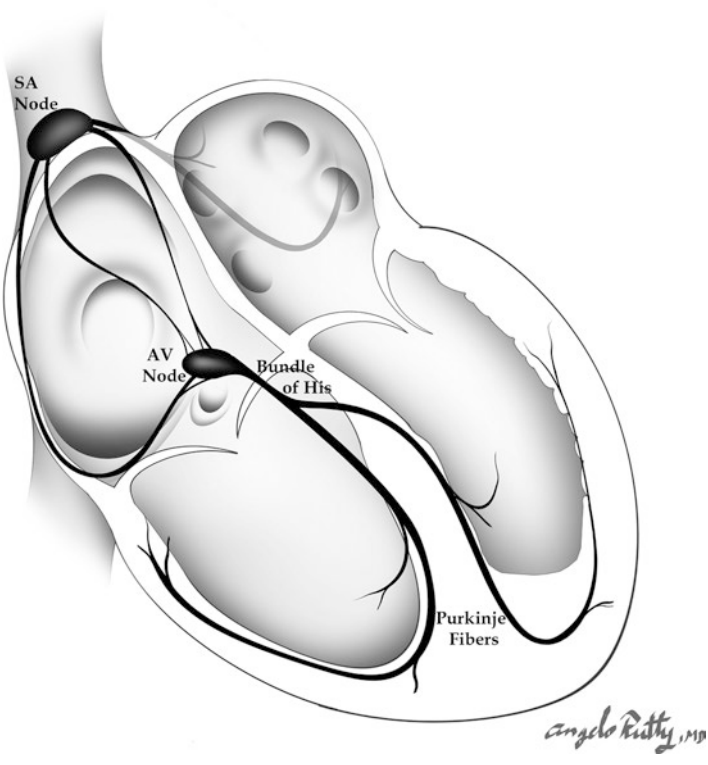

FIGURE 1.1 Diagrammatic representation of structures involved in normal cardiac conduction. *SA* sino-atrial, *AV* atrio-ventricular

is normally initiated by the sino-atrial (SA) node, a specialized group of myocardial cells in the high right atrium. These cells exhibit automaticity, meaning they spontaneously become electrically active (depolarize). The impulse then spreads to adjacent atrial myocytes via cell-to-cell connections termed gap junctions. Ultimately, the wave of depolarization reaches a second group of specialized cells at the bottom of the right atrium, near the crux of the heart, called the atrio-ventricular (AV) node. Because the atria and ventricles are electrically isolated from one another by a circumferential band of fibrous tissue at the level of the tricuspid and mitral valves, the

only path for impulse propagation is via the AV node. After a brief (approximately 0.1 s), intrinsic delay at the AV node, the action potential is propagated quickly down the bundle of His and Purkinje fibers within the ventricular myocardium. This rapidly conducting network acts as 'wiring' to convey the impulse to the apex of the heart, allowing for a coordinated, mechanically efficient contraction of the ventricles.

1.2.1 Action and Resting Potentials

At rest, cardiac myocytes maintain a net negative electrical gradient with respect to the extracellular environment (resting potential). The gradient results from the activities of ion channels and transporters within the cell membrane and is essential to the myocyte's (and heart's) ability to propagate electrical impulse. With sufficient stimulus, alterations in the myocyte's permeability to Na^+ result in a net positive electrical gradient with respect to the extracellular environment (depolarization). Further, changes in the myocyte's ion permeability to K^+, Cl^-, and Ca^{++}, result in the eventual restoration of the negative intracellular environment. When plotted against time, the changes in electrical potential are conventionally described as having five distinct phases (Fig. 1.2) which correspond to the stereotyped alterations in membrane permeability of the cardiac myocyte. Anti-arrhythmic medications exert their influence by altering membrane permeability, affecting the characteristics of the action potential. For example, class Ia agents (procainamide, disopyramide, and quinidine) affect Na^+ influx, resulting in a decreased rate of phase 0 depolarization and mild prolongation of repolarization [1].

1.2.2 Automaticity

Automaticity refers to the intrinsic ability of a cardiomyocyte or cluster of cells to spontaneously depolarize and thus initiate propagation of an action potential. Such cells are termed "pacemaker cells" and include those of the SA and AV nodes.

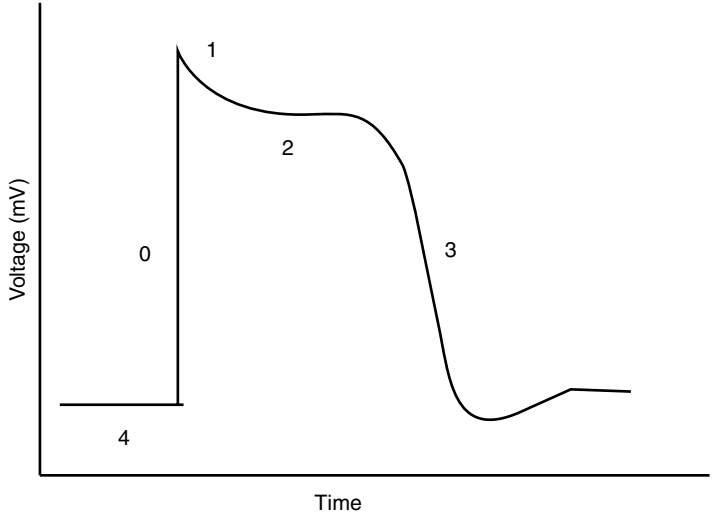

FIGURE 1.2 The action potential of a Purkinje fiber. Phase *4* is the resting state prior to electrical stimulation. Phase *0* is the rapid depolarization as a result of Na^+ influx. Phase *1* is the initial stage of repolarization due to closure of Na^+ channels and efflux of Cl^-. Phase *2*, or the plateau phase, is mediated primarily by Ca^{++} influx. Phase *3* is the rapid repolarization and is facilitated primarily by K^+ efflux. *mV* millivolts

Cells of the His-Purkinje system and even the ventricular myocardium may also spontaneously depolarize under circumstances of particularly slow cardiac rhythms (e.g., sinus node arrest, complete heart block). Because of the more rapid depolarization of the usual pacemakers, the automaticity of these cells is often not manifested during normal cardiac rhythm. Furthermore, after injury, cells which typically do not possess automaticity may acquire altered membrane conductance with resultant current leakage and spontaneous depolarization resulting in automatic tachycardias. Figure 1.3 depicts the action potential for cells of the SA and AV nodes. Notice the positively sloped phase 4, progressing toward threshold potential at which point phase 0 occurs. The slope of the phase 4 depolarization is a key determinant in the rate

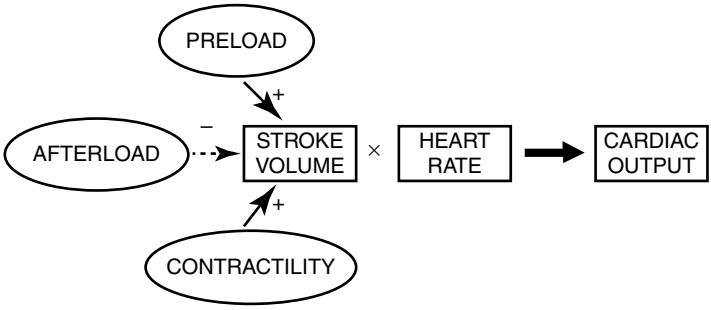

FIGURE 1.3 Preload, contractility, and afterload each impact cardiac output via their effects on stroke volume

of initiation of an action potential and thus overall heart rate. Modulation of automaticity occurs via the autonomic nervous system and may thus be affected by pharmacologic agents acting centrally (dexmedetomidine, clonidine) or those affecting the action potential initiation and propagation at the level of the myocytes (digoxin, beta-blockers). In clinical practice there is often an overlap of direct and autonomic effects with many pharmacologic agents.

1.2.3 Electromechanical Coupling

On a macroscopic level, propagation of the action potential from the high right atrium to the AV node, His-Purkinje system, and finally the ventricular myocardium allows for ordered, coordinated myocardial contraction and relaxation. On a cellular level, this is accomplished by coupling the changes in electrical environment to changes in mechanical activity (myocardial contraction and relaxation) via fluctuations of cytosolic Ca^{++} concentration. As a consequence of depolarization, cytosolic Ca^{++} concentration markedly increases via influx from the cell membrane as well as release of intracellular calcium stores within the sarcoplasmic reticulum. Ca^{++} directly enables the interaction of the contractile elements actin and myosin, the result of which is myofiber

shortening. Just as the process of myocyte contraction is reliant upon Ca^{++}, myocardial relaxation is an *active* process, requiring the expenditure of energy in the form of adenosine triphosphate (ATP) to scavenge Ca^{++} from the cytosol quickly and inhibit continued contraction [2]. The neonatal myocardium has a poorly developed calcium transport process which results in an exaggerated dependence upon extra-cellular calcium concentration to maintain cardiac contractility in neonates. For further detail on the downstream interactions between contractile elements and the process of electromechanical coupling, the reader is referred to selections referenced at the conclusion of this chapter.

1.2.4 Dysrhythmias

While an extensive review of all dysrhythmias is outside the scope of this chapter, a brief overview of the mechanisms of the basic categories of dysrhythmias is provided. On the simplest level, heart rhythm abnormalities can be divided into those that are 'too slow' (bradyarrhythmias) and those that are 'too fast' (tachyarrhythmias). Bradyarrhythmias primarily result from delay or block in conduction of the impulse from the high right atrium to AV node and His-Purkinje system, and most involve disease of the AV nodal tissue [first degree and second degree type I (Wenckebach) heart block] or of the His-Purkinje system [second degree type II (Mobitz) and third degree (complete) heart block]. Bradyarrhythmias may also result from disease of the sinus node (ineffective automaticity), such that no appropriate pacemaker is available to establish a physiologic heart rate. Tachyarrhythmias are more varied in terms of etiologies and can originate from the atria, ventricles, or AV node. However, the mechanism which underlies each can often be categorized as automatic or re-entrant. An automatic tachycardia results from a cell or cluster of cells acquiring abnormal automaticity, such that this region of the heart spontaneously depolarizes more rapidly than the sinus node, establishing the heart rate at greater than physiologic rates. The most common examples of automatic

tachycardias include ectopic atrial tachycardia, multifocal atrial tachycardia, and junctional ectopic tachycardia. Automatic tachycardias tend to exhibit a gradual 'warm-up' and/or 'cool-down' phases at onset and termination, and despite the overall rapid rate, there is subtle variability in heart rate over time. In contrast, re-entrant tachycardias result from additional, non-physiologic electrical pathways that allow conduction of an impulse to back to a region of the heart that has repolarized following the earlier conduction of the *same* impulse. Such 'short-circuits' essentially allow the same impulse to recycle itself and lead to successive depolarizations. Re-entrant tachyarrhythmias characteristically have an abrupt onset and termination and a non-varying rate during the tachycardia. The re-entrant circuit may exist exclusively within the atria (atrial flutter), ventricles (ventricular tachycardia), or AV node (AV node re-entrant tachycardia), or may be comprised of tissue that connects the atria, AV node, and/or ventricles (accessory pathway tachycardia).

1.3 Cardiovascular Physiology

Care of the patient with hemodynamic derangements remains rooted in basic physiologic concepts – preload, contractility, and afterload – first described in the late 19th century. These factors directly impact stroke volume, which along with heart rate are the key determinants of cardiac output (Fig. 1.4).

1.3.1 Preload

Preload refers to the ventricle's intrinsic ability, within a physiologic range, to alter the force of contraction based on the degree of ventricular filling just prior to contraction (end-diastolic volume/fiber length). The greater the end-diastolic volume, and thus ventricular myofiber stretch, the greater the force of contraction. This relationship of increasingly forceful contraction with increasing preload continues to correlate until the myocardial fibers are stretched to a point

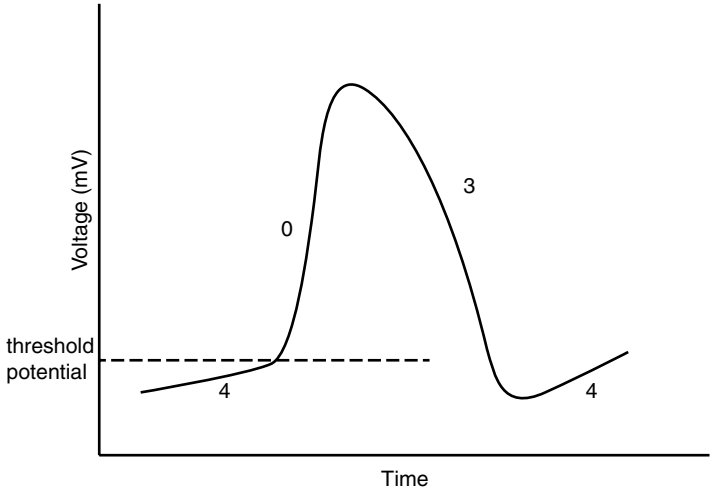

FIGURE 1.4 Diagrammatic representation of the action potential of sino-atrial or atrio-ventricular nodal cells. Phase *4* is characterized by the positive slope, indicating gradual depolarization toward threshold (termed automaticity), at which point the phase *0* upstroke is observed. *mV* millivolts. Phase *3* is repolarization phase returning the cell back to the baseline, or resting potential

that contractility actually begins to fall off. The relationship between preload and contractility is known as the Starling relationship. Conceptually, preload is most often equated with the intravascular volume status of a patient. Under conditions of relatively low volume status (e.g., dehydration), the force of myocardial contraction, and thus cardiac output, is diminished. Volume status is most often gauged clinically by measuring the central venous pressure (CVP), which is usually equivalent to the ventricular end-diastolic pressure. Assuming normal ventricular compliance (pressure-volume relationship) and absence of significant tricuspid (or mitral) stenosis, CVP is a clinically useful surrogate for preload. Caution must be used when interpreting the CVP in light of the clinical scenario (i.e., a 'normal' CVP may in fact be too low if there is a poorly compliant ventricle as occurs with diastolic dysfunction or constrictive pericarditis).

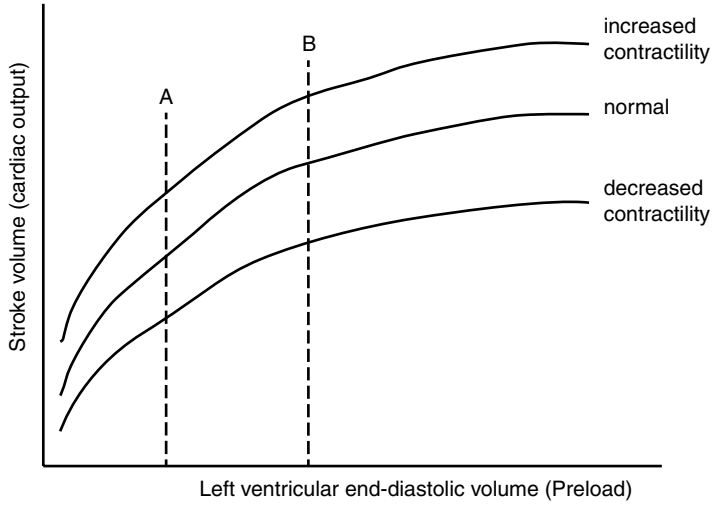

FIGURE 1.5 Frank-Starling curve illustrating the relationship between various preload, cardiac output, and inotropic states. At preload *A*, cardiac output is less than that at a greater preload *B*. However, for a given preload A or B, cardiac output is, in part, determined by the inotropic state (contractility)

1.3.2 Contractility

As already noted, within physiologic range, the greater the myofiber stretch (preload), the greater the force of contraction. However, contractility (or inotropic state) specifically refers to the magnitude of response to a given preload and can be thought of as the 'multiplication factor' for any given preload (Fig. 1.5). Contractility is an intrinsic property of the muscle fiber that is relatively independent of changes in preload or afterload. In other words, for any given preload, the force of contraction will be greater under conditions of increased inotropy (e.g., dobutamine infusion) and less under conditions of depressed inotropy (e.g., systolic dysfunction). In the setting of low cardiac output (e.g., dilated cardiomyopathy), improvement is sought by administration

of medication (e.g., dobutamine, low-dose epinephrine, milrinone, digoxin) to augment contractility. Each of these therapies has multiple effects, aside from enhanced inotropy, which may limit their therapeutic efficacy (e.g. increased myocardial oxygen consumption, excessive tachycardia, or arrhythmias).

1.3.3 Afterload

Afterload is defined as the ventricular wall stress during contraction and is often conceptualized as the load against which the ventricle contracts. In clinical practice, afterload is usually identified with systemic vascular resistance, which is primarily determined by the arteriolar resistance. However, from LaPlace's principle, wall stress is directly proportional not only to the ventricular pressure, but also to ventricular chamber diameter, while it is inversely proportional to ventricular wall thickness. Thus, for the left ventricle, the major components of afterload are peripheral vascular resistance, arterial wall stiffness, mass of the column of blood in the aorta, blood viscosity, and LV wall thickness and diameter. Similarly, for the right ventricle (RV), afterload is primarily influenced by pulmonary artery impedance, pulmonary vascular resistance, mass of the column of blood in the pulmonary circulation, viscosity of the blood, and RV chamber characteristics. Examples of clinical scenarios in which the left ventricle (LV) faces increased afterload include aortic stenosis (increased resistance), coarctation of the aorta and systemic hypertension (increased resistance and wall stiffness), and dilated cardiomyopathy (increased chamber diameter). For any given preload, greater afterload results in more limited myofiber shortening during contraction and decreased stroke volume as compared to contraction in the face of lesser afterload (see next section, SV_B vs. SV_{DA} of Fig. 1.5B). In other words, afterload determines the size of the ventricular cavity at the end of contraction, independent of the ventricular volume prior to contraction (preload).

1.3.4 Pressure-Volume Loops

Visual representations of these physiologic concepts can be helpful to appreciate best their individual characteristics and impact upon one another *in vivo*. One particularly useful way to appreciate the contributions of and interactions between preload, contractility, and afterload is by examination of pressure-volume loops. As shown in Fig. 1.6a, ventricular diastolic performance (compliance) and changes in preload are illustrated by the curve at the bottom of the graph, ventricular volume throughout the cardiac cycle is illustrated by the rectangle, and contractility is illustrated by the diagonal line at end-systolic volume (end-systolic pressure volume relationship). With the onset of systole (point A), there is an increase in pressure (isovolumic contraction) until ventricular pressure exceeds aortic pressure, at which point the aortic valve opens and blood is ejected from the ventricle (point B). As the ventricle continues to empty, there is the onset of relaxation of the ventricle with an eventual drop in pressure below that of the aorta (point C). At this point ventricular pressure falls but the volume remains unchanged (isovolumic relaxation) until the pressure drops below that of the left atrium and the mitral valve opens (point D). The ventricular volume then increases during diastole, until the cycle repeats itself with the next contraction. The area within the rectangle represents stroke work, and the distance along the x-axis between the vertical lines is the stroke volume. As illustrated in Fig. 1.6b, increased preload results in a greater stroke volume as compared to baseline, but the end-systolic volume in both instances is limited by the afterload (and contractility). With decreased afterload (dash-dot line), a lesser end-systolic volume and greater stroke volume are achieved. Conversely, increased afterload results in greater end-systolic volumes (i.e., decreased myofiber shortening) and diminished stroke volume. As shown in Fig. 1.6c, alterations in contractility (inotropic state) also affect changes in stroke volume. Finally, differences in ventricular compliance (slope and shape of curve at bottom of graphs) result in differences in end-diastolic volume (myofiber stretch) for a given preload (Fig. 1.6d), and thus also impact stroke volume.

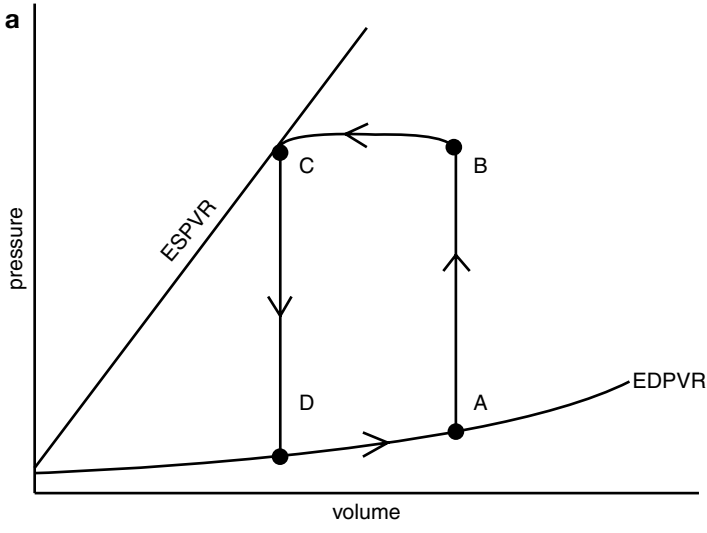

FIGURE 1.6 (**a**) Stylized pressure-volume loop. Followed in the counter-clockwise direction are end-diastolic volume and onset of systole (*A*), isovolumic contraction (*A–B*), aortic valve opening (*B*), ventricular ejection (*B–C*), aortic valve closure (*C*) and isovolumic relaxation (*C–D*), mitral valve opening (*D*) and diastolic filling of the ventricle (*D–A*). The volume difference between lines *AB* and *CD* is the stroke volume. *ESPVR* end-systolic pressure volume relationship, *EDPVR* end-diastolic pressure volume relationship. (**b**) Increased preload results in a greater stroke volume (SV_{IP}) as compared to baseline (SV_B), but the end-systolic volume in both instances is limited by the afterload (height of the PV curve) and contractility (slope of the ESPVR line). In the setting of decreased afterload, stroke volume is increased (SV_{DA}) by achieving a lower end-systolic volume. (**c**) For a given preload and afterload, stroke volume (*SV*) varies based on contractility. ESPVR lines *A*, *B*, *C* represent progressively increased inotropic states. (**d**) The impact of changes in ventricular compliance are depicted by the two EDPVR curves. In the setting of decreased compliance ($EDPVR_B$), a greater central venous pressure (CVP_B) is required to achieve the same ventricular end-diastolic volume and stroke volume (*SV*)

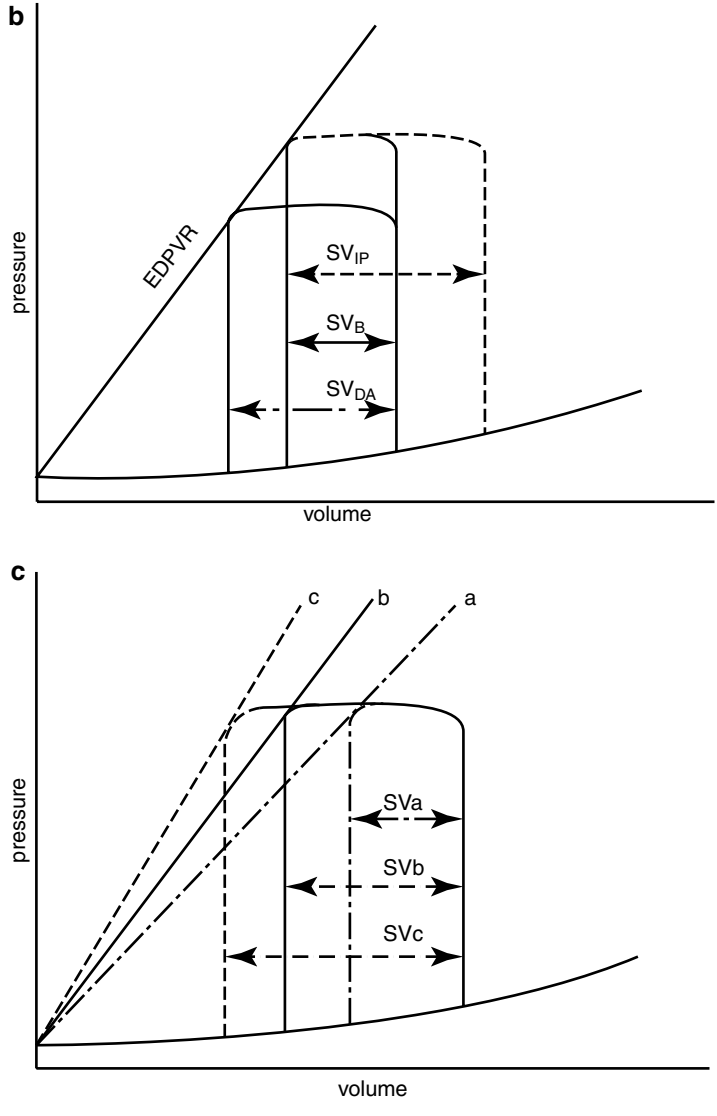

FIGURE 1.6 (continued)

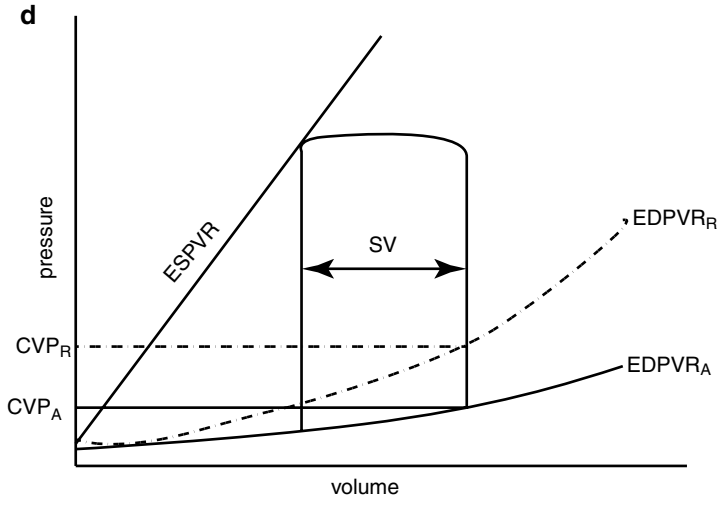

FIGURE 1.6 (continued)

1.3.5 Clinical Measures of Cardiac Function and Contractility

Bedside assessment and care of patients is driven in part by the technology available for clinical assessment. For example, while the use of impedance catheters to ascertain pressure-volume loops might best inform clinicians as to the changing cardiovascular status of their patients (and the response to therapies) during hemodynamic instability, this technology is impractical to use in most cases because they require an invasive procedure for placement and impractical levels of continuous monitoring. Thus, most clinicians rely on surrogate measures and their clinical experience to manage patients. Just as CVP is commonly used to estimate preload and systemic blood pressure to estimate afterload, echocardiographic assessments of ventricular systolic function are often relied upon to assess contractility. Specific estimators of contractility include shortening fraction (SF), ejection fraction (EF), and mean velocity of circumferential fiber shortening

(Vcfc). Both SF and EF are similar in their approach in that they measure the extent of shortening to assess LV systolic function. For EF, the end-systolic and end-diastolic parameters are estimated LV volumes (LVESV and LVEDV), whereas for SF, the parameters are linear measurements of LV cavity length or dimension (LVESD and LVEDD). The formulas for each are given below:

$$\mathrm{EF} = \left(\mathrm{LVEDV} - \mathrm{LVESV}\right) / \mathrm{LVEDV} \times 100$$

$$\mathrm{SF} = \left(\mathrm{LVEDD} - \mathrm{LVESD}\right) / \mathrm{LVEDD} \times 100$$

For EF the volumes are estimated from two dimensional echocardiography, whereas for SF the dimensions are measured using M-mode echocardiography. While both are relatively easy to ascertain and provide some quantification of LV systolic function, these measures are dependent on preload and afterload, which vary over time and are unlikely to be the same at serial evaluations. Another measure of ventricular function, mean Vcf_c, makes use of the rate of LV ejection to assess systolic function and has the advantage of being preload and heart rate independent, but still does not account for afterload.

Wall stress, the tension per unit cross-sectional area of myocardium, is thought to be the best estimator of ventricular afterload as it accounts for LV wall thickness (mass). Comparison of the mean Vcf_c to LV wall stress enables assessment of contractility free from the biases of preload, heart rate and afterload. Unfortunately, none of these measures account for ventricular diastolic function, an often underappreciated but increasingly recognized contributor to symptomatic heart failure. Indices of diastolic function are available but discussion of them is outside the scope of this chapter.

1.4 Unique Features of the Pediatric Heart

From structural, physiologic, and anatomic perspectives, the neonatal and pediatric heart differs from the adult heart. Animal studies have shown that both systolic and diastolic

cardiac function in the neonate are reduced compared to the adult. From a structural perspective, this results in large part from differences in calcium handling by the cardiomyocyte. Because the immature cardiomyocyte has less sarcoplasmic reticulum, intracellular calcium stores are limited [3]. The diminished numbers and activities of sarcoplasmic reticulum membrane transport proteins further differentiates the calcium flux of the immature heart from that of the adult heart. As a result of these differences in calcium handling, the immature cardiomyocyte has a greater reliance on extracellular calcium to enable myofibril contraction and relaxation [4]. Also contributing to the unique physiologic profile of the neonatal and infant heart are fewer numbers of contractile elements per myocyte and a greater relative proportion of non-cardiomyocytes to cardiomyocytes as compared to the mature heart. Additionally the alignment of the contractile elements of the neonatal heart is 'disorganized' when compared to the linear parallel arrangement of the contractile elements of the adult cardiomyocyte. The former likely impacts the ability to generate systolic tension, whereas the latter is thought to contribute to the relative non-compliance of the neonatal and infant heart.

Many of these structural differences impact the clinical characteristics of the neonatal and infant heart. For example, the neonatal and infant heart is exquisitely sensitive to serum calcium concentration, such that following cardiac surgery, calcium infusions are often used for inotropic support. Also, limited ventricular compliance results in the inability of neonates and young infants to augment stroke volume as a means of increasing cardiac output. Thus, the neonate, infant, and (to a lesser extent) the young child rely much more on increases in heart rate as the primary mechanism to augment cardiac output. Clinically, this explains the relatively fast heart rates of infants and young children, and the inability to tolerate heart rates that are normally observed in adults.

When evaluating a neonate, infant or young child, it is mandatory that a thorough assessment of the underlying cardiac anatomy be conducted, as significant structural lesions can go undetected prior to clinical presentation. Some of these

lesions result in heart failure from low cardiac output (e.g., left heart obstruction from coarctation of the aorta, hypoplastic left heart syndrome, or critical aortic stenosis), while others result in heart failure from pulmonary over-circulation (e.g., large left-to-right shunts from ventricular septal defects, or a patent ductus arteriosus).

1.5 Shunt Lesions and Calculations

Common to the practice of pediatric cardiology is the care of patients with structural lesions that cause shunting of blood. An explanation of the terms and calculations used to describe shunted blood flow follows. A key principle to keep in mind when considering congenital heart disease and quantification of shunts is that marked changes in systemic and pulmonary vascular resistance occur around the time of birth and continue for some time thereafter. These changes impact the direction and magnitude of shunt flow, and multiple therapeutic maneuvers (e.g., pharmacotherapy, mechanical ventilation, and inhaled gases) are often used to affect the degree and minimize the impact of shunting during the management of patients. It is also essential to appreciate the relationship that exists between cardiac output, vascular resistance, and blood pressure. This relationship is conceptualized as Ohm's Law (voltage = current × resistance) with the substitution of pressure (P) for voltage, cardiac output (Q), and vascular resistance (R) for current to yield the equation $\Delta P = Q \times R$.

As was noted at the onset of this chapter, the heart is in essence two pumps that are connected in series. The right heart pumps to the pulmonary circulation and the left heart to the systemic circulation. In the absence of a shunt, right heart cardiac output (Qp) is equal to left heart cardiac output (Qs), i.e., $Qp:Qs = 1$. In the setting of a net left-to-right shunt, $Qp:Qs > 1$, and in the setting of a net right-to-left shunt, $Qp:Qs < 1$. A simple rule of thumb (analogous to electrical current) is that 'blood flows down the path of least resistance'. Thus, the relative resistances

of the pulmonary and systemic circulations are a primary determinant of the net direction and magnitude of a shunt. Although this holds true for shunts at the ventricular (ventricular septal defects) and vascular levels (aortopulmonary window, patent ductus Arteriosus, and surgically created arterial shunts), the direction and magnitude of shunts at the atrial level are not determined by the downstream resistance, they are instead determined by the relative compliance of the left and right ventricles. In clinical practice, both flow and pressure are relatively easily measured, whereas resistance is usually calculated. Rearranging the equation noted above, pulmonary vascular resistance (PVR) = $\Delta P/Qp$, where ΔP is the transpulmonary gradient [mean pulmonary artery pressure – mean pulmonary vein (or left atrial) pressure]. Likewise, systemic vascular resistance (SVR) = $\Delta P/Qs$, where ΔP = transsystemic gradient [mean arterial pressure–central venous pressure].

In day–to-day practice, knowledge of the normal physiologic changes in PVR and SVR from fetus to neonate to adulthood enables clinicians to make reasonably valid assumptions about a particular patient's condition and to direct appropriate therapies. However, there are instances where the clinical picture is not entirely clear and quantification of the magnitude, or even net direction, of a shunt is necessary. Clinically, much of the information necessary to quantify a shunt or calculate resistance can be achieved at cardiac catheterization with the measurement of oxygen saturations and pressures in the various cardiac chambers and major blood vessels. Furthermore, quantification of Qp may be achieved at the bedside in the intensive care unit or at the time of catheterization with the use of a thermodilution catheter (i.e. Swann-Ganz catheter) or measurement of oxygen consumption (VO_2) and application of the Fick principle. While detailed descriptions of each of these techniques is outside the scope of this Handbook, a thermodilution catheter enables measurement of Qp and the pressures necessary to calculate PVR, whereas measurement of VO_2 and appropriateoxygen saturations enables calculation of Qp and Qs.

The reader is directed to the table at the end of this chapter for a list of commonly used formulas and to the suggested reference texts.

1.6 Hemodynamic Calculations

Example 1 – Large, unrestrictive ventricular septal defect in an 8 week old

	Pressure (mmHg)	Oxygen saturation (%)
Superior vena cava	8	68
Right ventricle	85/55	88
Pulmonary artery	70 (mean)	88
PCWP	15	98
Aorta	85/55	98

Hgb = 13.0 g/dL, VO_2 = 55.8 mL/min, and BSA = 0.25 m^2

Using Fick Equation:

$$\begin{aligned} Qp &= VO_2 / \left[\text{Hgb } (\text{g/dL}) \times 13.6 \times (PV_{sat} - PA_{sat}) \right] \\ &= 55.8 / \left[13 \times 13.6 \times (0.98 - 0.88) \right] = 3.2 \text{ L/min} \end{aligned}$$

$$\begin{aligned} Qs &= VO_2 / \left[\text{Hgb } (\text{g/dL}) \times 13.6 \times (Ao_{sat} - MV_{sat}) \right] \\ &= 55.8 / \left[13 \times 13.6 \times (0.98 - 0.68) \right] = 1.1 \text{ L/min} \end{aligned}$$

Thus, Qp:Qs = 3.2/1.1 ~ 3:1 (Alternately, since all other terms cancel out, if only saturations are known, can use $(Ao_{sat} - MV_{sat})/(PV_{sat} - PA_{sat}) = (0.98 - 0.68)/(0.98 - 0.88) = 3:1$).

$$Qp_i = Qp / BSA = 12.6 \text{ L/min/m}^2$$

$$\begin{aligned} PVR &= TPG / Qp_i = (70 - 15 \text{ mmHg}) / 12.6 \text{ L/min/m}^2 \\ &= 3.97 \text{ indexed Wood units} \end{aligned}$$

Example 2 – Large, unrestrictive ventricular septal defect in a 5 year old

	Pressure (mmHg)	Oxygen saturation (%)
Superior vena cava	8	68
Right ventricle	85/55	73
Pulmonary artery	70 (mean)	73
PCWP	15	98
Aorta	85/55	98

Hgb = 13.0 g/dL, VO_2 = 55.8 mL/min, BSA = 0.7 m^2

$$Qp_i = 5.0 \text{ L/min/m}^2$$

$$Qp : Qs = (0.98 - 0.68) / (0.98 - 0.73) = 1.2 : 1$$

Thus, $Qs_i = 5.0 \text{ L/min/m}^2 / 1.2 = 4.2 \text{ L/min/m}^2$

$$PVR = TPG / Qp_i = (70 - 15 \text{ mmHg}) / 5.0 \text{ L/min/m}^2$$
$$= 11.0 \text{ indexed Wood units}$$

Example 3 – Large atrial septal defect

	Pressure (mmHg)	Oxygen saturation (%)
Superior vena cava	10	72
Right atrium	10	79
Right ventricle	32/14	83
Pulmonary artery	20 (mean)	83
PCWP	11	99
Aorta	85/55	99

Hgb = 12.6 g/dL, VO_2 = 86 mL/min, BSA = 0.7 m^2

$$Qp_i = 4.48\,\text{L/min/m}^2$$

$$Qs_i = 2.65\,\text{L/min/m}^2$$

$$Qp : Qs = 4.48 / 2.65 = 1.69 : 1$$

$$PVR = TPG / Qp_i = (20 - 11\ \text{mmHg}) / 2.65\ \text{L/min/m}^2$$
$$= 3.4\ \text{indexed Wood units}$$

Example 4 – Tetralogy of Fallot

	Pressure (mmHg)	**Oxygen saturation (%)**
Right atrium	10	63
Right ventricle	85/55	63
Pulmonary artery	16 (mean)	63
PCWP	11	
Aorta	85/55	87

$Hgb = 14.2$ g/dL, $VO_2 = 62$ mL/min, $BSA = 0.3$ m^2

$$Qp_i = 2.97\,\text{L/min/m}^2$$

$$Qs_i = 4.43\,\text{L/min/m}^2$$

$$Qp : Qs = 2.97 / 4.43 = 0.67 : 1$$

$$PVR = TPG / Qp_i = (16 - 11\ \text{mmHg}) / 2.97\ \text{L/min/m}^2$$
$$= 1.68\ \text{indexed Wood units}$$

1.7 Formulas

$$Qp : Qs = \left(\frac{\text{aortic} - \text{mixed venous saturation}}{\text{pulmonary venous} - \text{pulmonary arterial saturation}} \right)$$

$$Qp = VO_2 / [13.6 \times Hgb\ (g/dL) \times (\text{pulmonary venous} - \text{pulmonary arterial saturation})]$$

$$Qs = CO = VO_2 / \left[13.6 \times Hgb\ (g/dL) \times (\text{aortic} - \text{mixed venous saturation})\right]$$

$$PVR = \text{transpulmonary gradient (TPG)} / Qp$$

$$TPG = \text{mean pulmonary artery pressure} - \text{pulmonary capillary wedge (or left atrial) pressure}$$

$$SVR = [\text{mean arterial pressure} - \text{central venous pressure}] / Qs$$

Further Reading

Colan SD. Assessment of ventricular and myocardial performance. In: Fyler DC, editor. Nadas' pediatric cardiology. Philadelphia: Hanley & Belfus; 1992. p. 225–48.

Fogoros RN. Practical cardiac diagnosis: electrophysiologic testing, third edition. Oxford: Blackwell Publishing; 1999. p. 1–33.

Lilly LS, editor. Pathophysiology of heart disease. Philadelphia: Lea & Febiger; 1993.

Mahony L. Development of myocardial structure and function. In: Allen HD, Gutgesell HP, Clark EB, Driscoll DJ, editors. Moss and Adams' heart disease in infants, children, and adolescents, 6th ed. Philadelphia: Lippincott Williams & Wilkins; 2001. p. 24–40.

Vargo TA. Cardiac catheterization: hemodynamic measurements. In: Garson A, Bricker JT, Fisher DJ, Neish SR, editors. The science and practice of pediatric cardiology, second edition. Baltimore: Williams & Wilkins; 1998. p. 961–93.

References

1. DiMarco JP, Gersh BJ, Opie LH. Antiarrhythmic drugs and strategies. In: Opie LH, Gersh BJ, editors. Drugs for the heart. 6th ed. Philadelphia: Elsevier Saunders; 2005. p. 218–9.

2. Schwartz SM. Cellular and molecular aspects of myocardial dysfunction. In: Shaddy RE, Wernovsky G, editors. Pediatric heart failure. Boca Raton: Taylor & Francis Group; 2005. p. 71–3.
3. Fisher DJ. Basic science of cardiovascular development. In: Garson A, Bricker JT, Fisher DJ, Neish SR, editors. The science and practice of pediatric cardiology. Baltimore: Williams and Wilkins; 1998. p. 201–9.
4. Ralphe JC. Pathophysiology of chronic myocardial dysfunction. In: Slonim AD, Pollack MM, editors. Pediatric critical care medicine. Philadelphia: Lippincott Williams & Wilkins; 2005. p. 230–4.